ELSEVIER

European Journal of Cardio-thoracic Surgery 29S (2006) S115—S125

EUROPEAN JOURNAL OF CARDIO-THORACIC SURGERY

www.elsevier.com/locate/ejcts

Septal structure and function relationships parallel the left ventricular free wall ascending and descending segments of the helical heart

Nikola Hristov [a], Oliver J. Liakopoulos [a], Gerald D. Buckberg [a,b,*], Georg Trummer [a]

[a] *Department of Surgery, Division of Cardiothoracic Surgery, David Geffen School of Medicine at University of California Los Angeles, 10833 Le Conte Avenue, 62-258 CHS, Los Angeles, CA 90095-1701, USA*

[b] *Option on Bioengineering, California Institute of Technology, Pasadena, CA, USA*

Received 17 February 2006; accepted 27 February 2006

Abstract

Objective: Determine if ventricular septum structure and function relationships parallel the left ventricular free wall descending and ascending segments of the helical heart. **Methods:** Forty pigs (30—38 kg) were studied physiologically by sonomicrometer to determine if septal fiber orientation resembled responses in the free wall. Following pilot studies in the non-bypassed heart, a right ventriculotomy was made to place septum crystals with fiber orientations that were either perpendicular to or reflected simultaneous free wall measurements. Postbypass measurements tested responses to positive (dopamine) and negative (esmolol) inotropic agents. **Results:** Similar oblique fiber directions were found for baseline percent systolic shortening (SS%) in the free wall and septum; free wall descending and ascending SS% were $21 \pm 3\%$ and $10 \pm 3\%$, and $13 \pm 2\%$ and $12 \pm 2\%$, respectively, in the septum. Conversely, impaired shortening occurred when transverse fiber direction was tested. Both oblique areas demonstrated comparable time-delay changes between free wall and septal descending and ascending segment at onset (75 ± 11 ms) and termination (86 ± 21 ms) of contraction. Dopamine increased heart rate and caused a similar increase of free wall descending and ascending segment SS% to $24 \pm 2\%$ and $14 \pm 3\%$ ($p < 0.05$), and septal SS% response to $16 \pm 2\%$ and $15 \pm 2\%$ ($p < 0.05$), and comparable decrease of time-delay changes of shortening between ascending and descending segments of 54 ± 6 ms and 68 ± 10 ms, respectively ($p < 0.05$). Conversely, esmolol decreased heart rate and similarly reduced SS% in left ventricular free wall (descending: $18 \pm 4\%$; ascending: $7 \pm 4\%$; $p < 0.05$) and septum (descending: $10 \pm 2\%$; ascending: $10 \pm 3\%$; $p < 0.05$). Time-delay of contraction between segments was increased to 91 ± 4 ms ($p < 0.05$), but the hiatus at the end of shortening remained unchanged, due to prolonged endocardial contraction. **Conclusions:** Septal structure and function relationships parallel the left ventricular free wall ascending and descending segments, thereby supporting the helical heart fiber spatial relationships. The oblique fiber orientation may make the septum become the '*lion of right ventricular function*'.

Keywords: Heart anatomy; Ventricular septum; Helical heart; Ventricular myocardial band; Sonomicrometry

1. Introduction

The ventricular septum is a thick structure comprised of discrete muscular bands that separates the left and right ventricles, and contributes to cardiac function. Analysis of this structure and function relationship requires a full understanding of how anatomic form translates into hemodynamic performance, but this interface has not yet been determined. Consequently, we currently continue to follow the 1790 projections of Weber [1], who indicated that actions of muscular heart would not be understood until the muscle bundles of the septum are clarified.

Septal studies are traditionally separated into anatomic and physiologic frameworks. However, insight into the interaction of the different muscular components that spatially form the ventricular mid-wall is needed to determine mechanisms of form and function to explain sequential cardiac events. The helical cardiac configuration was initially described over 500 years ago [2], together with extensive recent anatomic studies that separate cardiac muscle into superficial sinospiral and deep bulbospiral structures [3]. Unfortunately, the classic reports by Pettigrew et al. [4] did not distinguish how the oblique septal fibers (Fig. 1A) that interact to form the ventricular vortex, can coordinate to produce the twisting and untwisting action described so elegantly in (a) the visual images from Mall's anatomic report in 1911 [3] (Fig. 1B) and (b) more recently in vivo by MRI analyses [5,6].

Progress toward clarifying septal anatomy came from Greenbaum et al. [7] whose cross sections demonstrated oblique criss-cross endocardial and epicardial fibers containing a circumferential mid-septal wall (Fig. 2A), and from Lunkenheimer et al.'s [8] elegant use of computerized tomographic scans to define the interweaving collagen

* Corresponding author. Tel.: +1 310 206 1027; fax: +1 310 825 5895.
E-mail address: gbuckberg@mednet.ucla.edu (G.D. Buckberg).

1010-7940/$ — see front matter © 2006 Elsevier B.V. All rights reserved.
doi:10.1016/j.ejcts.2006.02.041

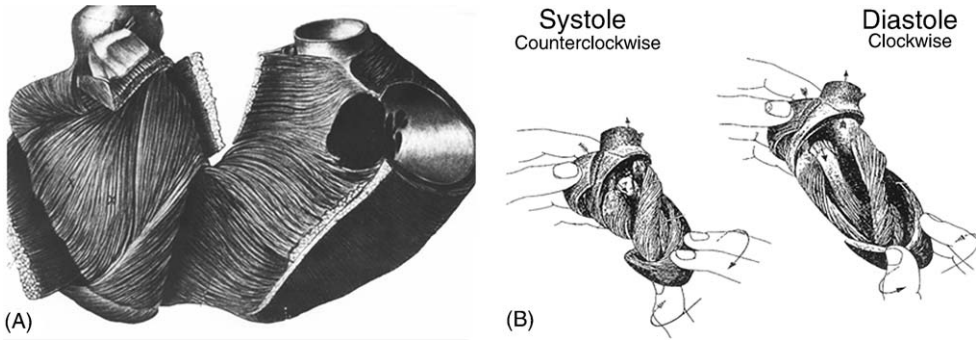

Fig. 1. Anatomic figure shown by Mall [3] published in 1911 where (A) ventricular septum fibers course in oblique directions, and (B) ventricular twisting is postulated to exist in counterclockwise direction during systole (left) and clockwise direction during diastole (right). Note the fixed position of the apex and the spiral arrangements of muscle fibers from base to apex.

support of the connective tissue skeleton that likely is the scaffold of reciprocally oblique septal muscular fibers (Fig. 2B).

Torrent-Guasp described the ventricular myocardial band in a helical heart that is composed of basal and apical loops [9,10,11]. The basal loop of the unraveled band contains transverse fibers that wrap around the right and left ventricles (Fig. 3). The apical loop, when folded, contains oblique fibers that include the septum that is comprised of descending and ascending segments, and a ventricular vortex at the apical tip. Lunkenheimer initially used Torrent-Guasp's dissections [8] to provide necropsy definition of the reduplicating oblique septal scaffold for septal muscular components, but he and Anderson no longer accept the Torrent-Guasp model [12–15].

Physiologic studies continued despite lack of precise anatomic confirmation of septal morphology, and evaluated how measurements of cavity volume, pressures, and systolic and diastolic wall stresses influenced septal impaction upon normal and abnormal functions [16]. Imaging considerations sometimes report right- and left-sided septal structures, and differ from the anatomic recommendations of Greenbaum [7], whose observations suggested the septum belongs to the left ventricle because of his necropsy analysis of how endocardial right- and left-sided fibers interacted with the circumferential fibers. Conversely, the physiologic studies of Klima et al. [17,18] defined how the septum might determine the magnitude of left ventricle–right ventricle interaction, and demonstrated how interruption of septal anatomy by coagulation would predominantly impair right ventricular function. This principal right ventricular detrimental action was further clarified by Agarwal et al. [19] following isolated ischemia of the interventricular septum. Santamore and Dell'Italia [16] reported a clear in-depth analysis of how the septum influenced physiologic aspects of ventricular interdependence.

Connection of physiology to function requires analysis of contractile shortening of the left and right sides of the thick septum, with findings based upon an anatomic framework. This study tests a hypothesis that the septum reflects the underlying structure of the free left ventricular wall, because it is comprised of the same descending and ascending segments of the apical loop configuration described by Torrent-Guasp et al. [10,11]. Accumulated information shall satisfy the objectives of (a) identifying the dominant angle of maximal muscular contraction on thick septal left and right septal sides, (b) defining a similar sequential shortening pathway as exists within the thick left ventricular free wall, and (c) clarifying a comparable response to positive and negative inotropic influences. The validity of findings may fulfill the existent gap in knowledge about septal anatomy and function.

2. Materials and methods

All animals received humane care in compliance with the 1996 NRC Guide for the Care and Use of Laboratory Animals,

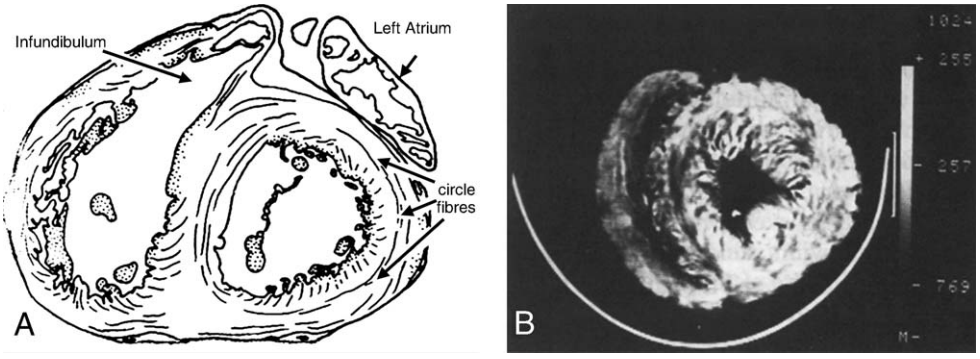

Fig. 2. (A) Greenbaum's cross-sectional images that demonstrate the oblique criss-cross endocardial and epicardial fibers contained within a circumferential mid-septal wall (from Greenbaum et al. [7], published in 1981). (B) Lunkenheimer's computerized tomographic scans demonstrating the interweaving collagen support of the connective tissue skeleton that is likely the scaffold for reciprocally oblique septal muscular fibers (from Lunkenheimer et al. [8], published in 1984).

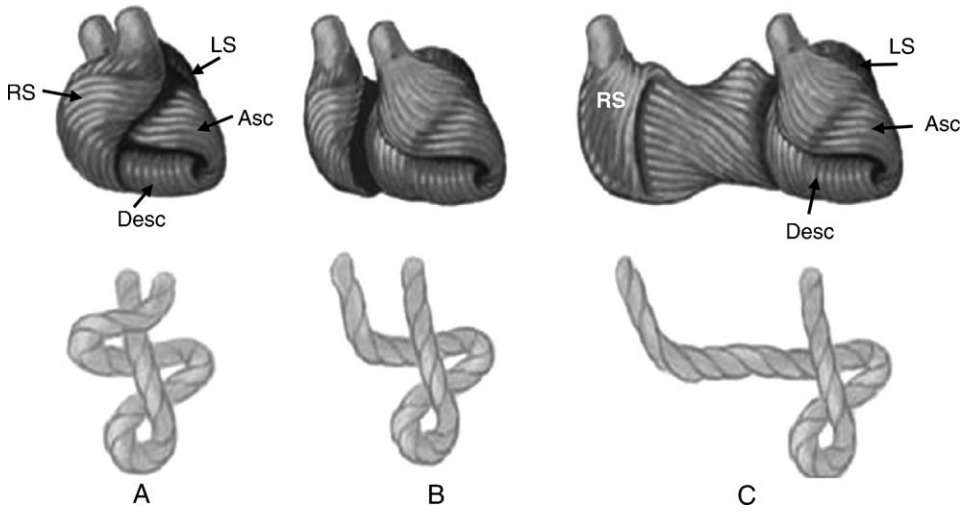

Fig. 3. Schematic drawings of the progressive unfolding of the ventricular myocardial band in comparison with underlying rope-like model. Note (A) the intact heart, (B) detachment of the pulmonary artery with unfolding of the basal loop right segment (RS), and (C) complete unfolding of the basal loop RS that reveals the underlying oblique orientated descending (Desc) and ascending (Asc) segment of the septum and LV free wall. LS: left segment of basal loop.

available at: http://www.nap.edu/readingroom/books/labrats/contents.html.

Ten early studies were done without bypass, and 30 subsequent studies were done using extracorporeal circulation to allow direct septal visualization.

Forty Yorkshire–Duroc pigs (29.5–38.4 kg) were premedicated with ketamine hydrochloride (15 mg/kg) and diazepam (0.5 mg/kg) intramuscularly and anesthetized with inhaled isoflurane 1.5% (MAC 1%). Support with a volume-controlled ventilator (Servo 900C, Siemens-Elema, Sweden) was started after tracheotomy and endotracheal intubation. The left extrathoracic mammary artery was cannulated for arterial pressure measurement and blood gas analysis. Arterial blood gases were measured to keep oxygen tension, carbon dioxide tension and pH values in normal range. A balloon-tipped pulmonary artery catheter (Model 132F5, Baxter Healthcare Corp., Irvine, CA, USA) was inserted through the right subclavian vein to measure cardiac output (thermodilution technique) and pulmonary artery pressure. Each pig underwent median sternotomy, and exposure of the heart, following a pericardial incision.

Thirty pigs underwent systemic heparinization (300 units/kg), and a 12 F arterial cannula (Medtronic Inc., Minneapolis, MN, USA) was inserted into the superficial femoral artery, and two 17 F venous cannulas (Medtronic Inc.) were inserted into the superior and inferior vena cava through the superficial jugular vein and femoral vein, respectively. Extracorporeal circulation was instituted using a membrane oxygenator (Affinity NT 541, Medtronic Inc.) and an extracorporeal pump (Sarns, Ann Arbor, MI, USA) with the circuit primed with 1000 ml Plasma-Lyte solutions (Baxter Healthcare Corp.), 700 ml stored porcine packed blood, and calcium chloride for normocalcemia (1.0–1.2 mmol/l). Cardiopulmonary bypass (CPB) was started at 300 mmHg oxygen tension, 50–70 mmHg arterial pressure, and flow adjustment to keep ~70% mixed venous oxygen saturation and 35–37 °C rectal temperature.

A solid-stated pressure transducer-tipped catheter (Model MPC-500, Millar Instruments Inc., Houston, TX, USA) was inserted via the left ventricular apex for left ventricular hemodynamic measurements. Arterial pressure (AP), left ventricular pressure (LVP), dP/dt, and sonomicrometer crystals data were digitally processed by specific hardware and software (Sonometrics, London, Ont., Canada). Regional shortening was measured with pairs of 2 mm ultrasonic microtransducer crystals (Sonometrics).

Percentage of segmental shortening (SS%) was calculated as follows

$$\frac{\mathrm{EDL} - \mathrm{ESL}}{\mathrm{EDL}} \times 100$$

where EDL is end-diastolic length and ESL is end-systolic length.

Velocity of sound through cardiac tissue was fixed to 1590 m/s. Sonomicrometer measurements were recorded with a sampling rate of 195.8 samples/s, a transmitter spacing of 652 μs, transmit inhibit delay of 1.18 μs, and transmit pulse length of 375 ns. Synchronicity between myocardial shortening was compared to left ventricular performance with 5 ms precision. All studies were performed and analyzed by the same surgeon.

2.1. Septal approach

Figs. 3–7 define the anatomic considerations underlying this effort to record sonomicrometer crystal tracings from the left and right ventricular aspects of the septum. The bias was that (a) unfolding the right ventricular free wall (Figs. 3 and 4) will expose the helical septum constructed from overlap of the oblique left-sided descending segment and a right-sided ascending segment of the helical heart apical loop; (b) the dominant shortening direction should conform to vectors of crystal placement confirmed in left ventricular free wall (Figs. 5–7) [20]; and (c) sequential performance of this muscular septal infrastructure will parallel the sequential shortening sequence in the LV free wall caused by positive and negative inotropic interventions.

The challenge of obtaining satisfactory sonomicrometer tracings of septal activity required a series of 40 studies that

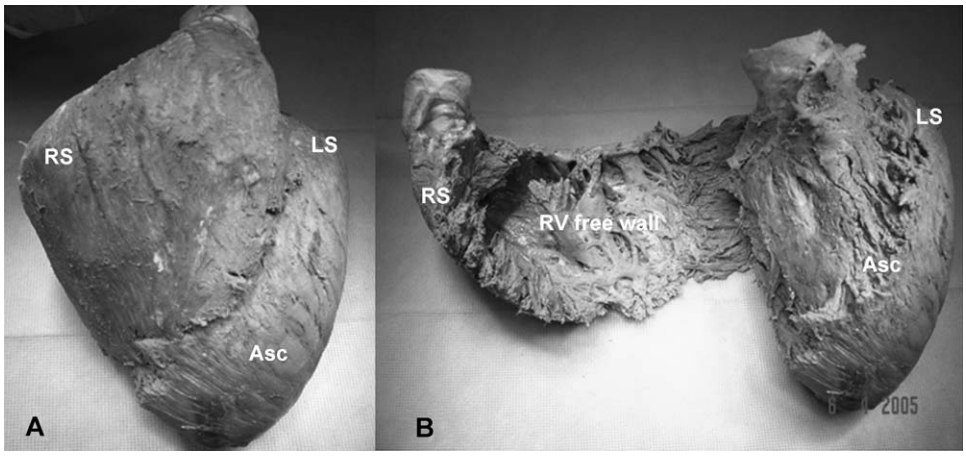

Fig. 4. Anatomic preparations showing the orientation of the ventricular myocardial band of the (A) intact heart and (B) after exposing the septum by unfolding of the right ventricle free wall. Note the similar configuration of the septum and LV free wall composed of the ascending segment of the apical loop. RS: right segment of basal loop; LS: left segment of basal loop; Asc: ascending segment of apical loop.

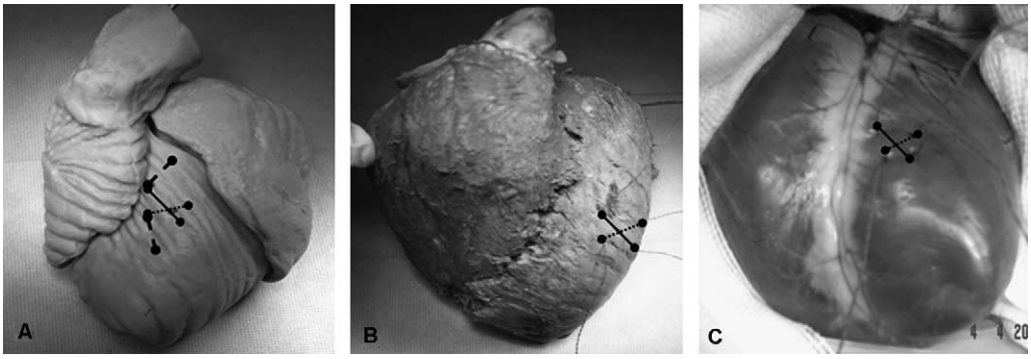

Fig. 5. Helical heart model (A), anatomic specimen (B), and experimental study (C) showing sonomicrometer crystal positioning in the descending and ascending segments of the left ventricular free wall. Crystal orientation was either in the direction of left ventricular free wall maximal segmental shortening of descending (●- - -●) and ascending segments (●—●), or placed perpendicular (●- -●) to maximal segmental shortening position (in (A)).

ranged from non-bypassed heart, cardiopulmonary bypass with and without cardioplegia, and evaluation of biventricular versus right ventricular approaches. This evolution is summarized so that those who seek to repeat these attempts can recognize the problems of obtaining sonomicrometer recordings from a thick intraventricular muscle that is surrounded by the thick and thin free walls of the left and right heart.

A basic requirement is satisfactory recording of sequential shortening of the descending and ascending segments of the left ventricular free wall. The logic is related to (a) prior LV free wall studies [20] establishing the correct angulation of

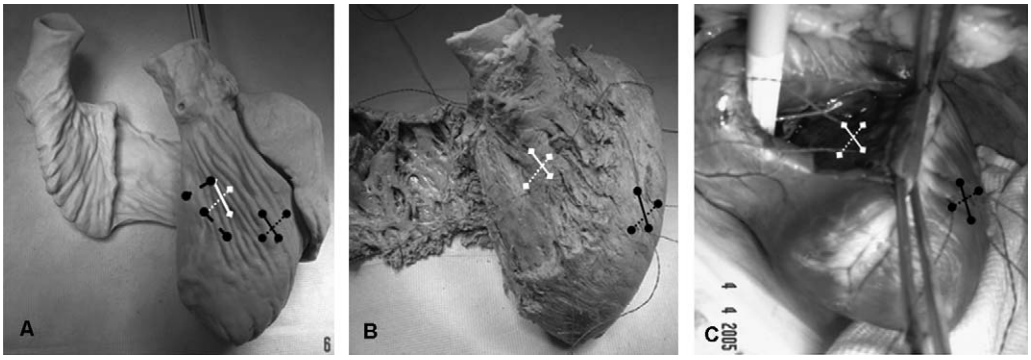

Fig. 6. Helical heart model (A), anatomic specimen (B) and experimental study (C) of the septum and LV free wall to demonstrate sonomicrometer crystal positioning. Crystal orientation was in direction of maximal segmental shortening of descending (●- - -●) and ascending segments (●—●) of left ventricular free wall and septum descending (■- - -■) and ascending segments (■—■), and placed in a perpendicular direction (●- -●) to septal maximal segmental shortening (in (A)).

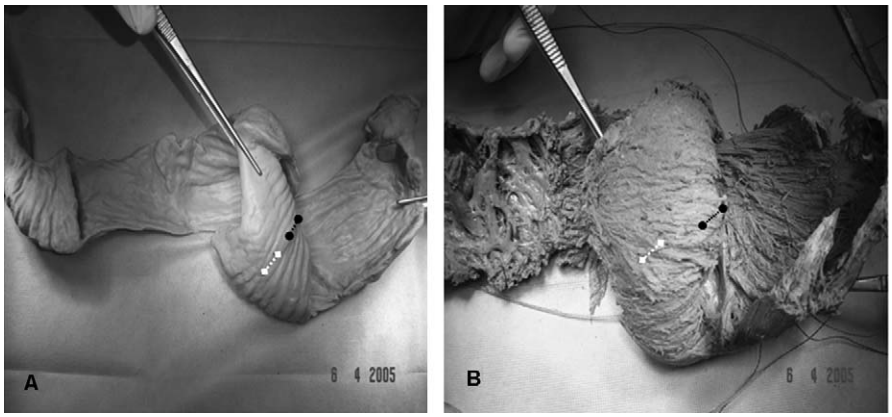

Fig. 7. Helical heart model (A) and anatomic specimen (B) of the septum and LV free wall to demonstrate sonomicrometer crystal positioning of the descending segment. The region is exposed by unfolding its attachment to the ascending segment. Note the parallel crystal orientation angulation of the septal (■- - -■) and LV free wall (●—●) descending segment in direction of the fiber orientation of the descending segment of the apical loop.

crystal placement (Figs. 5 and 6), and (b) testing this bias by comparison of free wall records to septal tracings. Failure to make this correlation invalidates the hypothesis of this experiment.

2.2. Without CPB

Two methods were tested and involved either (a) approaching the septum surface on the outside surface of the right and left ventricular sides, or (b) transmurally via septal muscle penetration by an external blind approach (via the free LV and RV walls).

Initial studies used the free wall of the left and right ventricles to advance crystals into the respective cavity (confirmed by back bleeding) with subsequent septal surface penetration on either side. Free wall angulation positions were used as guidelines for satisfactory positions. Despite good initial recordings, these site locations were transient. Consequently, either crystal fixation by suture or impaction against the underlying septum (as with free wall endocardial placement) was needed to sustain the position.

Secondary efforts used transmural crystal placement by advancing a longer insertion sheath to cross the septum flowing free wall insertion, and then withdrawing it to endocardially attach crystals on the right and left ventricular septal sides. Constant recordings could not be obtained and postmortem studies showed improper positioning. These inconsistent findings led to subsequent direct septal vision studies.

2.3. With CPB

The first study addressed the left- and right-sided septums by direct vision via a 4 cm ventriculotomy on the left and right sides. The beating heart was used and crystals were placed on left and right septal endocardium to avoid transmural changes due to multiple septal punctures. Placement angulation was either in an oblique pathway along the free wall fiber direction pathway (Fig. 6) or in a transverse direction and across the expected maximum shortening direction as reported previously [20].

Each crystal was fixed with a prolene stay suture, but the direction of suture placement effected results. Initially satisfactory recordings failed after transverse suture placement, as this positioning compressed underlying oblique fibers, whereas oblique direction suture placement allowed consistent and satisfactory left- and right-sided septal tracings.

Despite valid recordings in the open ventricle, consistent irregular left-sided recordings occurred after discontinuation of bypass for subsequent measurements. The need for repeat left ventriculotomy for replacement of crystals created an unsatisfactory solution because new septal damage occurred after many repetitive septal punctures.

A second study used a brief interval of hyperkalemic cardioplegia to expedite ventriculotomy, crystal placement, and closure. These studies were also unsuccessful because initial assessment of correct function was delayed until ventricular closure, which often resulted in dislocation of crystals.

The third study was successful, as only a 4 cm right ventriculotomy was used to approach both sides of the septum (Figs. 5 and 6). Left-sided septum crystals were placed via a transmural puncture (similar to transmural epicardial procedure used to place free wall endocardial crystals) with a specially designed PVC tube, and right-sided endocardial crystals were inserted just beneath the RV septal surface. All data were collected following right ventriculotomy closure and discontinuation of bypass.

2.4. Experimental protocol

Each pig underwent placement of two pairs of sonomicrometer crystals on the epicardial and endocardial sides of the left ventricular free wall (Fig. 5). These baseline free wall tracings were then compared to septal crystal tracings. On the free wall epicardial side, crystals were placed beneath a 1 mm epicardial incision. Endocardial crystals were then placed by inserting a specific crystal introducer (1 mm diameter PVC tube) beyond the 1 mm epicardium incision into the ventricular cavity (identified by pulsatile bleeding), the sensor cord was then pulled against the endocardial surface with subsequent epicardial fixation by a 4/0 Prolene

suture. Postmortem examination confirmed LV surface and septum position.

Local heart coordinates were used to select highest point at aortic annulus, and lowest at the apex. A North and South fashion was used to define the crystal placement angles for most powerful segmental shortening as described previously [20]. Epicardial crystal angles were between 140° and 150°, compared to between 80° and 90° (Fig. 5) for endocardial sites.

After free wall crystal placement, CPB was initiated and total bypass was achieved by snaring the inferior and superior cava veins. A beating heart was always used, and the 3—4 cm right ventriculotomy was made parallel to the left anterior descending artery. Following placement of free wall traction sutures, the RV septum underwent placement of 4/0 Prolene stay sutures for crystal placement.

The ascending segment forms the right ventricular side of the septum [10,21] and three crystals were placed in two angulation directions. One orientation site followed the specific oblique ascending segment fiber orientation, while the other direction was perpendicular to the free wall ascending segment fiber direction (Fig. 6).

The descending segment forms predominantly the left ventricular side of the septum, and was approached via the right ventricular side of the septum. Following the 1 mm incision, a 1 mm diameter PVC crystal introducer tube was pushed into the left ventricular cavity. Pulsatile bleeding confirmed the transmural position, and crystals were brought to septal endocardial wall by pulling on the electrical cord wire to place the sensor against the LV septum. As with the right side, placement was done in a direction along the descending segment fibers, and then perpendicular to them (Figs. 6 and 7). The right ventricle was closed with a 2/0 Prolene suture and CPB was slowly discontinued.

Baseline hemodynamic measurements and crystal recordings were performed 15 min after weaning from CPB. Responses to positive and negative inotropic agents were subsequently recorded after administering (a) dopamine at 10 μg/(kg min) and (b) a 50 mg esmolol bolus injection after the dopamine effect subsided.

2.5. Statistical analysis

Hemodynamic and sonomicrometer data were compared by *t*-test between pharmacologic interventions and are reported as mean ± standard deviation (mean ± SD). *p*-values <0.05 were considered statistically significant.

3. Results

Hemodynamic stability existed before, during, and after bypass, with a mean arterial pressure of 71 ± 14 mmHg before CPB, 59 ± 8 mmHg during CPB, and 68 ± 9 mmHg at post-CPB measurements. Mean heart rate was 74 ± 23 beats/min before CPB, 82 ± 12 beats/min during CPB, and 78 ± 17 beats/min after bypass, and cardiac output measured before pharmacologic intervention averaged at 2.2 ± 0.2 l/min during the entire post-CPB period.

Baseline LV free wall SS% were 21 ± 3% and 10 ± 3% for the descending and ascending segments, respectively, and SS% of the septal descending and ascending segments were 13 ± 2% and 12 ± 2%, respectively (Table 1). These tracings displayed the expected 75 ± 11 ms time-delay between the start of descending and ascending segment shortening. Similarly, a 86 ± 21 ms hiatus existed between the end of ascending segment shortening and the earlier completion of descending segment shortening (Fig. 8; Table 2). As described below, a similar pattern of delays between the initiation and termination of contraction of the left and right sides of the septum exited, but timing and magnitude depended upon the positioning of the paired crystals.

Table 1
Percentage of segmental shortening (SS%) of the descending and ascending segments in the left ventricular free wall and ventricular septum at baseline, after dopamine (10 μg/(kg min)) and esmolol (50 mg) administration

	Baseline (%)	Dopamine (%)	Esmolol (%)
Left ventricular free wall			
Descending segment	21 ± 3	24 ± 2*	18 ± 4*
Ascending segment	10 ± 3	14 ± 3*	7 ± 4*
Ventricular septum			
Descending segment	13 ± 2	16 ± 2*	10 ± 2*
Ascending segment	12 ± 2	15 ± 2*	10 ± 3*

Data are mean ± SD.
* $p < 0.05$ compared to baseline values.

Septal recordings were first done in the open beating heart on CPB to (a) compare with the LV free wall, and (b) confirm the proper septal descending and ascending segments position of crystals. Positioning of the crystals perpendicular to the septum ascending and descending directions yielded different time intervals and markedly reduced SS%, thus emphasizing that maximal SS% evolves

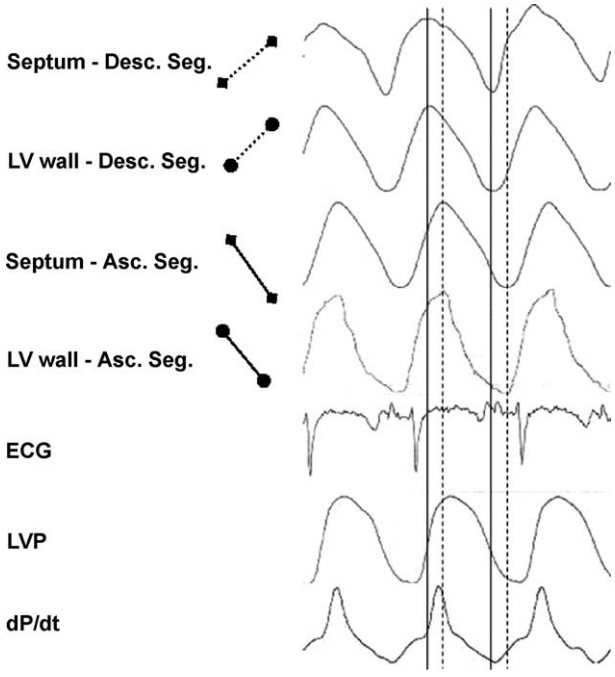

Fig. 8. Simultaneous segmental shortening recordings from LV free wall and septum. Note the similar and simultaneous start and end of contraction of the descending segment in the LV free wall and septum (solid line), and the similar and simultaneous start and end of contraction of the ascending segment in the LV free wall and septum (hatched line).

Table 2
Time-delay at the start and end of contraction between the descending (Desc) and ascending (Asc) segment at baseline, after dopamine (10 μg/(kg min)) and esmolol (50 mg) administration

	Baseline	Dopamine	Esmolol
Heart rate (beats/min)	82 ± 12	105 ± 9*	69 ± 9*
Time-delay start of contraction (descending–ascending segment) (ms)	75 ± 11	54 ± 6*	91 ± 5*
Time-delay end of contraction (descending–ascending segment) (ms)	86 ± 21	68 ± 10*	83 ± 7

* $p < 0.05$ compared to baseline values.

from correct placement of the septal descending and ascending segments (Fig. 9).

Conversely, this disparity between the time-delays and quantification of shortening disappeared when crystal placement followed the direction of the fibers of the descending and ascending segment as shown in Fig. 8. Analysis showed that after septal crystal placement within fiber direction that paralleled free wall, fibers displayed a 75 ± 11 ms time-delay between initiation of contraction of the descending and ascending segments. Additionally, a time-delay of 86 ± 21 ms was observed between the end of descending and subsequent ascending segment shortening. No LV hemodynamic parameters were obtained because these measurements were performed on CPB and during open right ventriculotomy.

After baseline measurements, dopamine was administered at 10 μg/(kg min) which resulted in an increase of heart rate from 82 ± 12 beats/min to 105 ± 9 beats/min ($p < 0.05$; Table 1; Fig. 10). The time-delay between the start of contraction in the descending and ascending segments decreased from 75 ± 11 ms to 54 ± 6 ms ($p < 0.05$), and the duration hiatus between the descending and ascending segment at end of contraction was shortened from 86 ± 21 ms to 68 ± 10 ms ($p < 0.05$; Table 2; Fig. 10). Left ventricular free wall SS% increased to 24 ± 2% and 14 ± 3% at the descending and ascending segments, respectively, and significantly exceeded baseline SS% ($p < 0.05$). Similarly, septal contractility increased to 16 ± 2% and 15 ± 2% at the descending and ascending segments, respectively ($p < 0.05$ vs baseline; Table 1).

Esmolol administration, given after the dopamine effect had subsided, decreased heart rate to 69 ± 9 beats/min, depressed SS% significantly in all segments as shown in Table 1, and prolonged the time-delays of the start of the contraction between the descending and ascending segments from 75 ± 11 ms to 91 ± 5 ms ($p < 0.05$ vs baseline; Table 2, Fig. 10). Esmolol prolonged endocardial contraction, so that the time hiatus between end of ascending and descending segment contraction was not prolonged (compared to baseline recordings), despite the slower heart rate.

4. Discussion

The hypothesis was testing if the function capacity of the helical rope-like model concept of Torrent-Guasp et al. [10,11] could solve the previously absent structure and function relationship of the ventricular septum. Achievement of positive findings may challenge established anatomical concepts of myocardial structure that underlie

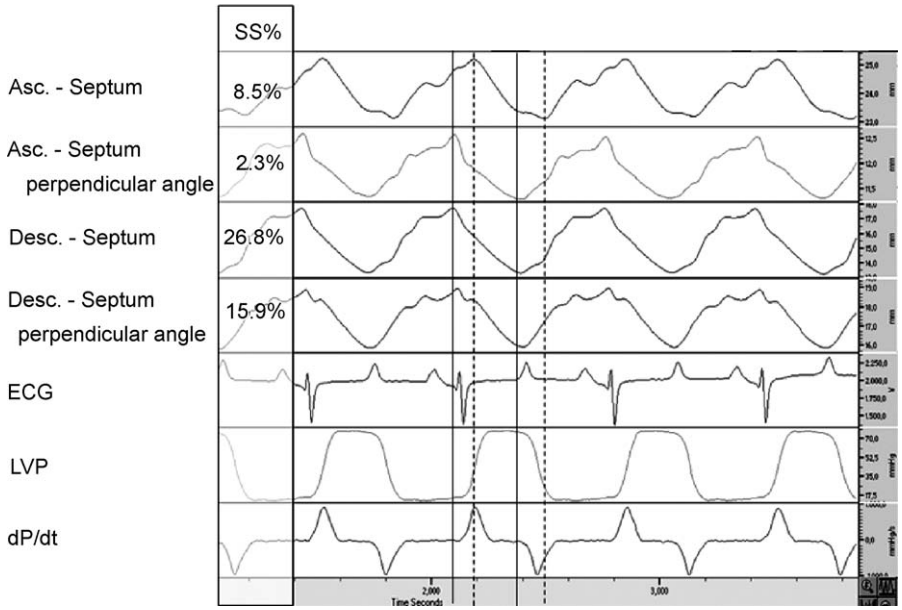

Fig. 9. Simultaneous segmental shortening recordings from the septal ascending (hatched line) and descending segment (solid line) and from septal crystals in an oblique transverse (perpendicular) direction to maximal SS%. Note that transverse placement of crystals resulted in (a) a significant decrease in SS%, and (b) and parallel shortening to the apical loop segments, indicating a tear from the ascending and descending segment during shortening. ECG: electrocardiogram; LVP: left ventricular pressure; d*P*/d*t*: first derivate of LVP.

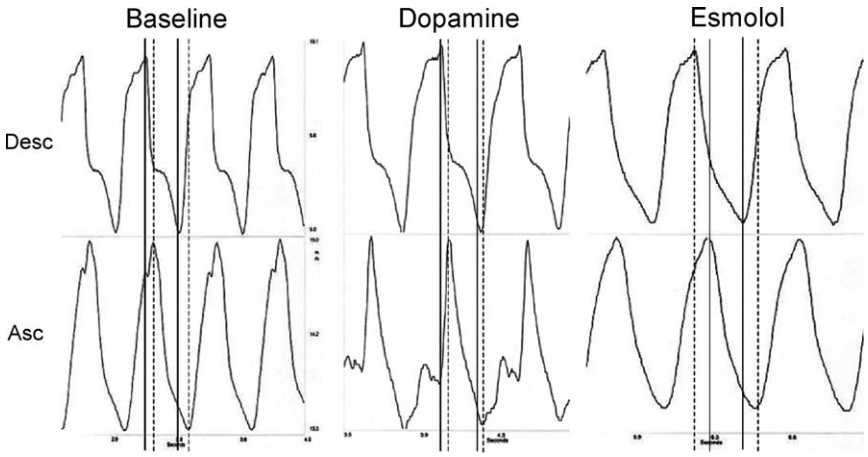

Fig. 10. Representative example of SS% sequence of the septal ascending and descending segment at baseline, and after administration of dopamine and esmolol. Note the change of time-delay at start of contraction between the descending and ascending segment at baseline, and after dopamine (10 μg/(kg min)) and esmolol (50 mg) administration (Table 2). Solid line: beginning and end of contraction of the descending segment; hatched line: beginning and end of contraction of the ascending segment.

function, since this spatial architectural model offers a radically different appreciation of heart anatomy and physiology.

The study was biased, since the experimental design was geared to evaluate: (a) if the septum had a spatial configuration that matched the helical ascending and descending segments of the apical loop that was presumed to form it, (b) if the major septal shortening sequence pattern existed within fiber orientation pathways that followed those preciously established in the left ventricular free wall [20], and (c) if septal muscle displayed a similar response to positive and negative inotropic drugs to confirm the contractile nature of active diastolic filling from isovolumetric contraction (rather than conventional isovolumetric relaxation). Each goal was accomplished to provide a novel septal structure and function relationship.

Analysis of dominant shortening characteristics along the fiber orientation within the ventricular myocardial band model of myocardial structure requires evaluation of the validity of the rationale behind the experimental design. The helical rope like model consists of a single muscle band that extends from below the pulmonary artery to form a basal loop that wraps transversely around the right and left ventricles, undergoes a spiral ventricular myocardial fold to become a helix composed an oblique descending segment, apical vortex and reciprocal oblique ascending segment to finish at the trigones of the aorta.

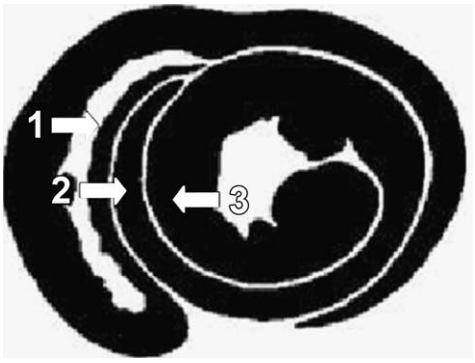

Fig. 11. Schematic drawing of the three muscular strata that constitute the interventricular septum: (1) recurrent fibers stratum, (2) ascending segment stratum, and (3) descending segment stratum.

The septum is thus surrounded by the right ventricular segment of the basal loop, and when exposed (Fig. 11), is made from three muscular strata [10] that include: (a) the right stratum represented by oblique fibers of right ventricular free wall, which turn towards inside of the ventricle and cover subendocardially the right ventricular side of the septum after reaching the anterior interventricular surface, (b) the middle stratum consisting of oblique fibers of ascending segment, and (c) the left stratum composed of oblique fibers of the descending segment.

Emphasis is placed upon the obliquity of the helical ascending and descending fibers, since correct angulation of crystal placement orientation within the septal ascending and descending segments was needed to determine if maximal segment shortening could be compared to established findings in the left ventricular free wall. Recent studies by Gorodkov et al. [22] used ventricular corrosion casts to display how spiral fibers compressed blood to provide further confirmation of oblique trabeculae. Additionally, MRI analysis of strain and velocity by Jung et al. [23] defined an oblique systolic shortening velocity, together with a similar reciprocal acceleration velocity during ejection, as a functional supplement to septal oblique fiber orientation.

Septal transverse or oblique directions were tested to determine timing and extent of maximum shortening. The oblique direction was essential (Figs. 5, 6 and 8) and confirmed the hypothesis. Furthermore, tracing distortion occurred when stay sutures were placed in transverse rather than oblique position, thereby confirming the importance of the oblique angulation. Conversely, failure to reproduce free wall findings would invalidate the hypotheses. Furthermore, understanding this design bias clarifies why (a) sonomicrometer crystals were used to address how ascending and descending segments formed the left and right sides of septum, and (b) studies on and off bypass were done with use of the beating heart, cardioplegia, and biventricular and

right ventricular approaches, to evolve the confirmatory data that comprises this report.

The heart undergoes sequential activation of the ventricular band to produce four cardiac movements which include: (a) narrowing by contraction of outer basal loop and internal surface of the descending segment, (b) shortening by co-contraction of the predominant descending and then ascending segments of the apical loop, (c) lengthening by unopposed contraction of the ascending segment of the apical loop, and (d) relaxation without contraction of any part of the myocardial band. Theoretical form animation of this sequence is seen on the web site http://www.gharib.caltech.edu/, under helical heart. These four movements explain both phases of cardiac function, including co-contraction for systolic ejection, and unopposed ascending contraction to allow the active muscular early suction phase for rapid ventricular filling; an action that differs from the conventional acceptance of elastic recoil from stored potential energy during systole to explain isovolumetric relaxation [5,24].

Reproduction of left ventricular free wall studies was essential to match with the septum, and current findings confirmed previous sequential movements causing systolic ejection and early suction phase of the diastolic cardiac function [20]. This is shown in Fig. 8, demonstrating (a) simultaneous early shortening of descending segment of the free wall and septum, (b) later origin of ascending segment shortening in free wall and septum, (c) co-contraction of descending and ascending segments of free wall and septum during ejection, (d) ongoing ascending shortening in free wall and septum during rapid fall in left ventricular pressure, just before when active suction occurs, and (e) similar delay between end of descending segment shortening and later completion of ascending shortening.

These interactions produce the following physiologic results relative to septal contributions to cardiac action. The co-contraction following shortening of both the descending and ascending segments of the septum allows the whole septum to contribute to longitudinal shortening of the ventricle during systolic ejection, which is associated with clockwise twisting on MRI analysis [5,6]. The ascending segment continues to shorten after the descending segment stops to allow suction for rapid filling, thereby using the descending segment as a fulcrum to lengthen during the rapid fall in the ventricular pressure curve [25]. The suction phase of the cardiac cycle is characterized by reciprocal twisting to accentuate rapid filling [25].

The observed role of the septum in cardiac anatomic morphology now interfaces with its dominant role in heart physiology and function. Reproduction of prior free wall findings related to ejection and suction following positive and negative inotropic drug administration [20] confirmed the calcium related muscular components of septal action. Dopamine produced tachycardia, increased SS%, and decreased the time-delay between descending and ascending sequences of shortening. Conversely, beta blockade with esmolol decreased heart rate and SS%, increased the time-delay between the beginning of the contraction of the descending and ascending segments, and preferentially delayed relaxation of the septal endocardial descending segment to impede rapid filling.

Ventricular suction normally occurs during the duration hiatus between the end of shortening of the descending and ascending segments, so that restriction of this hiatus by a negative inotropic agent at a lower heart rate would interfere with suction. Indirect evidence of this comes from a slower down slope of the left ventricular pressure curve and less negative dP/dt [20]. The dynamic effect of less vigorous relaxation and this observation serves as a keynote into diastolic dysfunction; more filling pressure is needed when a negative inotropic influence impairs suction.

Dell'Italia [26] in 1991 observed that despite markedly different muscle mass and chamber geometry, both ventricles are bound together by remarkable spiral muscle bundles that encircle them in a complex interlacing fashion that includes the septum to form a highly interdependent functional unit. The septum, together with the left ventricle free wall, is the basic structural components of the left ventricle. The anatomic components of the right ventricle functional performance are the external free wall and internal septum [27,16]. Forces are transmitted from one ventricle to another through the septum, independently of the neural, humoral and circulatory effects [16]. These effects are immediate, on beat-to-beat basis, and they are known as ventricular interdependence [16]. The septum is a key element for ventricular interaction, now shown to have oblique fiber orientation in the helical heart model, and this central structure predominantly contributes to the normal shortening and lengthening of the ventricles during cardiac cycle that produces systolic ejection and also contributes to the early suction phase of rapid ventricular filling [28,29].

4.1. Fiber orientation and septal function

During normal cardiac action, MRI studies confirm that the predominant heart motions include twisting for clockwise ejection and reciprocal twisting for suction [5,6]. These motions are determined by fiber orientation. Sallin [30] and Ingels [24] report that ejection fraction is ~60% with oblique orientation, and reduced to ~30% after transverse or horizontal fiber orientation. The sonomicrometer studies evaluated maximum shortening and confirm the oblique maximum direction of fiber orientation in septum and free wall of the normal ventricle. While crystal shortening reflects local dimensional changes in only the limited region studied, this action likely underlies the transmural twisting of ventricular movements responsible for ejection and suction.

Recorded oblique septum and free wall observations differ from prior right ventricular sonomicrometer studies [20] showing a transverse, rather than oblique orientation of basal loop fibers that wrap around the right ventricle. Functional constriction or narrowing follows this horizontal orientation, accounting for isometric cardiac compression that narrows the mitral valve annulus during this pre-ejection interval [31]; a cocking or counterclockwise motion [32] event that results from the horizontal basal loops shortening during this early isometric phase of the cardiac cycle. In contrast, longitudinal septal motion predominantly contributes to ventricular shortening during ejection and lengthening during suction, so that oblique fiber direction accounts for clockwise twisting during right ventricular ejection. This differs from the left ventricle, where systolic clockwise

twisting occurs in both the septum and left ventricle free wall to generate high systemic pressure during normal left-sided ejection.

Physiologic consequences follow restriction of the oblique pattern responsible for twisting to the septum, since the right-sided basal loop has predominantly transverse fibers. This transverse fiber configuration during basal loop contraction leads to circumferential compression, which adequately maintains right-sided ejection with normal pulmonary artery pressure. However, loss of septal twisting will accentuate right ventricular failure if there is pulmonary hypertension. These observations are linked to the importance of functional oblique septal fibers, and imply that the septum should be considered the '*lion of right ventricular function*'.

Fiber orientation and functional observations have clear impact during cardiac surgery, as septal hypokinesia or akinesia is a common finding [33—35] which may reflect stunning caused by impaired myocardial protection [36]. Iatrogenic loss of the septal twisting responsible for generating adequate RV function with pulmonary hypertension thereby provides insight into causative reasons for clinical difficulty in correcting right heart failure. This new knowledge about septal fiber orientation and its interaction with right heart failure may focus future investigations upon evaluation of septal function, and underscore development of protective methods that avoid this complication. Iatrogenic septal damage is consistent with Klima et al.'s [17] and Agarwal et al.'s [19] observations that define how septal paralysis impairs right heart function.

Subsequent systolic function can also be markedly altered by changes in septal anatomy that result from diastolic septum stretching. For example, distension will distort fiber orientation thereby creating a more horizontal pattern [37,16] that differs from the normal curvilinear septal shape that protrudes into the right ventricle. Septal stretch alters the normal oblique septal fiber orientation toward a more transverse or horizontal position, and then changes left and right heart hemodynamics; this event creates 'an architectural disadvantage' that relates to functional alterations produced by septal displacement.

This anatomic underpinning is introduced to explain ventricular interdependence, whereby myocardial factors determine how one ventricle affects the performance of the other ventricle. Bernheim [38] in 1910 described right ventricular compression after left ventricular hypertrophy, and Dexter [39] in 1956 described a 'reverse Bernheim event' after large atrial septal defects and right-sided volume overload. These changes in contralateral ventricular function are now amended by adverse septal stretch following left-sided dilation from ischemic [40], valvular [41], and non-ischemic cardiomyopathy [42], or from right septal stretch following extensive left ventricular decompression following LVAD insertion [43] or pulmonary hypertension [44].

5. Conclusions

Experimental evaluation of septal structure and function relationships with sonomicrometer crystal measurements shows how fiber orientation determines the maximum rate of systolic shortening, and validates the hypothesis that septal anatomy conforms to the descending and ascending segments of the ventricular myocardial band. This basic spatial configuration underlies the apical loop component of the helical heart, as described by Torrent-Guasp. Oblique fibers of the endocardial regions of the left and right sides of the septum displayed the same functional characteristics that exist in the free left ventricular wall, and thereby confirm a comparable spatial structural configuration. The muscular components of co-contraction for ejection and active and unopposed ascending contraction for rapid ventricular filling were verified, and similar time-related sequences of shortening and lengthening for rapid filling existed, while the septum and free wall responded comparably to positive and negative inotropic drugs.

The predominantly oblique architecture of septal muscle likely governs the twisting cardiac action during ventricular ejection, compared to the transverse fiber structure of basal segment of the free right ventricular wall. These normal functional events were related to reciprocal oblique fiber orientation comprising the septum, and mechanisms of impaired septal performance were suggested when pathologic lesions disrupted the fiber orientation of septal architecture. These observations further suggest that the septum might be considered the '*lion of right ventricular function*' in patients with pulmonary hypertension.

References

[1] Weber EH. Hilderbrand's Handbuch der Anatomie des Menschen, 4th Edition. Leipzig; 1831.
[2] Lower R. Tractus de Corde 1669. Early Science in Oxford. Oxford: Sawsons; 1932.
[3] Mall FP. On the muscular architecture of the ventricles of the human heart. Am J Anat 1911;11:211—78.
[4] Robb JS, Robb RC. The normal heart: anatomy and physiology of the structural units. Am Heart J 1942;23:455—67.
[5] Rademakers FE, Buchalter MB, Rogers WJ, Zerhouni EA, Weisfeldt ML, Weiss JL, Shapiro EP. Dissociation between left ventricular untwisting and filling. Accentuation by catecholamines. Circulation 1992;85(4):1572—81.
[6] Shapiro EP, Rademakers FE. Importance of oblique fiber orientation for left ventricular wall deformation. Technol Health Care 1997;5(1—2):21—8.
[7] Greenbaum RA, Ho SY, Gibson DG, Becker AE, Anderson RH. Left ventricular fibre architecture in man. Br Heart J 1981;45(3):248—63.
[8] Lunkenheimer PP, Muller RP, Konermann C, Lunkenheimer A, Kohler F. Architecture of the myocardium in computed tomography. Invest Radiol 1984;19(4):273—8.
[9] Torrent-Guasp F. The cardiac muscle Madrid, Spain: Fundacin Juan; 1973.
[10] Torrent-Guasp F, Buckberg GD, Clemente C, Cox JL, Coghlan HC, Gharib M. The structure and function of the helical heart and its buttress wrapping. I. The normal macroscopic structure of the heart. Semin Thorac Cardiovasc Surg 2001;13(4):301—19.
[11] Torrent-Guasp F, Ballester M, Buckberg GD, Carreras F, Flotats A, Carrio I, Ferreira A, Samuels LE, Narula J. Spatial orientation of the ventricular muscle band: physiologic contribution and surgical implications. J Thorac Cardiovasc Surg 2001;122(2):389—92.
[12] Anderson RH. Systolic ventricular filling. Eur J Cardiothorac Surg 2004;26(2):461—2.
[13] Lunkenheimer PP, Redmann K, Dietl KH, Cryer CW, Richter KD, Whimster WF, Niederer P. The heart's fibre alignment assessed by comparing two digitizing systems. Methodological investigation into the inclination angle towards wall thickness. Technol Health Care 1997;5(1—2):65—77.
[14] Lunkenheimer PP, Redmann K, Scheld H, Dietl KH, Cryer C, Richter KD, Merker J, Whimster W. The heart muscle's putative "secondary structure". Functional implications of a band-like anisotropy. Technol Health Care 1997;5(1—2):53—64.

[15] Lunkenheimer PP, Redmann K, Anderson RH. The architecture of the ventricular mass and its functional implications for organ-preserving surgery. Eur J Cardiothorac Surg 2005;27(2):183—90.
[16] Santamore WP, Dell'Italia LJ. Ventricular interdependence: significant left ventricular contributions to right ventricular systolic function. Prog Cardiovasc Dis 1998;40(4):289—308.
[17] Klima U, Guerrero JL, Vlahakes GJ. Contribution of the interventricular septum to maximal right ventricular function. Eur J Cardiothorac Surg 1998;14(3):250—5.
[18] Klima UP, Lee MY, Guerrero JL, Laraia PJ, Levine RA, Vlahakes GJ. Determinants of maximal right ventricular function: role of septal shift. J Thorac Cardiovasc Surg 2002;123(1):72—80.
[19] Agarwal JB, Yamazaki H, Bodenheimer MM, Banka VS, Helfant RH. Effects of isolated interventricular septal ischemia on global and segmental function of the canine right and left ventricle. Am Heart J 1981;102(4):654—8.
[20] Castella M, Buckberg GD, Saleh S, Gharib M. Structure function interface with sequential shortening of basal and apical components of the myocardial band. Eur J Cardiothorac Surg 2005;27(6):980—7.
[21] Buckberg GD, Coghlan HC, Torrent-Guasp F. The structure and function of the helical heart and its buttress wrapping. V. Anatomic and physiologic considerations in the healthy and failing heart. Semin Thorac Cardiovasc Surg 2001;13(4):358—85.
[22] Gorodkov A, Dobrova NB, Dubernard JPH, Kiknadze GD, Gatchetchiladze IA, Oleinikov VG, Kuzmina NB, Barat JL, Baquey CH. Anatomical structures determining blood flow in the heart left ventricle. J Mater Sci 1996;7:153—60.
[23] Jung B, Schneider B, Markl M, Saurbier B, Geibel A, Hennig J. Measurement of left ventricular velocities: phase contrast MRI velocity mapping versus tissue-doppler-ultrasound in healthy volunteers. J Cardiovasc Magn Reson 2004;6(4):777—83.
[24] Ingels Jr NB. Myocardial fiber architecture and left ventricular function. Technol Health Care 1997;5(1—2):45—52.
[25] Buckberg GD, Clemente C, Cox JL, Coghlan HC, Castella M, Torrent-Guasp F, Gharib M. The structure and function of the helical heart and its buttress wrapping. IV. Concepts of dynamic function from the normal macroscopic helical structure. Semin Thorac Cardiovasc Surg 2001;13(4):342—57.
[26] Dell'Italia LJ. The right ventricle: anatomy, physiology, and clinical importance. Curr Probl Cardiol 1991;16(10):653—720.
[27] Buckberg GD, Coghlan HC, Hoffman JI, Torrent-Guasp F. The structure and function of the helical heart and its buttress wrapping. VII. Critical importance of septum for right ventricular function. Semin Thorac Cardiovasc Surg 2001;13(4):402—16.
[28] Buckberg GD. Architecture must document functional evidence to explain the living rhythm. Eur J Cardiothorac Surg 2005;27(2):202—9.
[29] Torrent-Guasp F, Kocica MJ, Corno A, Komeda M, Cox J, Flotats A, Ballester-Rodes M, Carreras-Costa F. Systolic ventricular filling. Eur J Cardiothorac Surg 2004;25(3):376—86.
[30] Sallin EA. Fiber orientation and ejection fraction in the human left ventricle. Biophys J 1969;9(7):954—64.
[31] Ormiston JA, Shah PM, Tei C, Wong M. Size and motion of the mitral valve annulus in man. I. A two-dimensional echocardiographic method and findings in normal subjects. Circulation 1981;64(1):113—20.
[32] Lorenz CH, Pastorek JS, Bundy JM. Delineation of normal human left ventricular twist throughout systole by tagged cine magnetic resonance imaging. J Cardiovasc Magn Reson 2000;2(2):97—108.
[33] Chouraqui P, Rabinowitz B, Livschitz S, Horoszowsky D, Kaplinsky E, Smolinsky A. Effects of antegrade versus combined antegrade/retrograde cardioplegia on postoperative septal wall motion in patients undergoing open heart surgery. Cardiology 1997;88(6):526—9.
[34] Okada RD, Murphy JH, Boucher CA, Pohost GM, Strauss HW, Johnson III G, Daggett WM. Relationship between septal perfusion, viability, and motion before and after coronary artery bypass surgery. Am Heart J 1992;124(5):1190—5.
[35] Waggoner AD, Shah AA, Schuessler JS, Crawford ES, Nelson JG, Miller RR, Quinones MA. Effect of cardiac surgery on ventricular septal motion: assessment by intraoperative echocardiography and cross-sectional two-dimensional echocardiography. Am Heart J 1982;104 (6):1271—8.
[36] Castella M, Buckberg GD, Tan Z, Ignarro LJ. Systolic and diastolic dysfunction in stunned myocardium and its prevention by Na^+—H^+ exchange inhibition. Eur J Cardiothorac Surg 2006 [in this supplement].
[37] Buckberg GD, Coghlan HC, Torrent-Guasp F. The structure and function of the helical heart and its buttress wrapping. VI. Geometric concepts of heart failure and use for structural correction. Semin Thorac Cardiovasc Surg 2001;13(4):386—401.
[38] Bernheim D. De l'asystolie veineuse dans l'hypertrophie due coer gauche par stenose concomitante du ventricule droit. Rev Med 1910;39:785.
[39] Dexter L. Atrial septal defect. Br Heart J 1956;18:209.
[40] Burch GE, Giles TD, Martinez E. Echocardiographic detection of abnormal motion of the interventricular septum in ischemic cardiomyopathy. Am J Med 1974;57(2):293—8.
[41] Young AA, Orr R, Smaill BH, Dell'Italia LJ. Three-dimensional changes in left and right ventricular geometry in chronic mitral regurgitation. Am J Physiol 1996;271(6):H2689—700.
[42] Suma H, Isomura T, Horii T, Buckberg G. Role of site selection for left ventriculoplasty to treat idiopathic dilated cardiomyopathy. Heart Fail Rev 2004;9(4):329—36.
[43] Moon MR, Bolger AF, DeAnda A, Komeda M, Daughters GT, Nikolic SD, Miller DC, Ingels Jr NB. Septal function during left ventricular unloading. Circulation 1997;95(5):1320—7.
[44] Agata Y, Hiraishi S, Misawa H, Takanashi S, Yashiro K. Two-dimensional echocardiographic determinants of interventricular septal configurations in right or left ventricular overload. Am Heart J 1985;110(4): 819—25.